Ice Surface Temperature, Ice Concentration, and Ice Cover Algorithm Theoretical Basic Document

Technical Report · December 2015

2 authors:

Yinghui Liu
University of Wisconsin–Madison
39 PUBLICATIONS **567** CITATIONS
SEE PROFILE

Jeffrey Robert Key
National Oceanic and Atmospheric Administr…
215 PUBLICATIONS **4,711** CITATIONS
SEE PROFILE

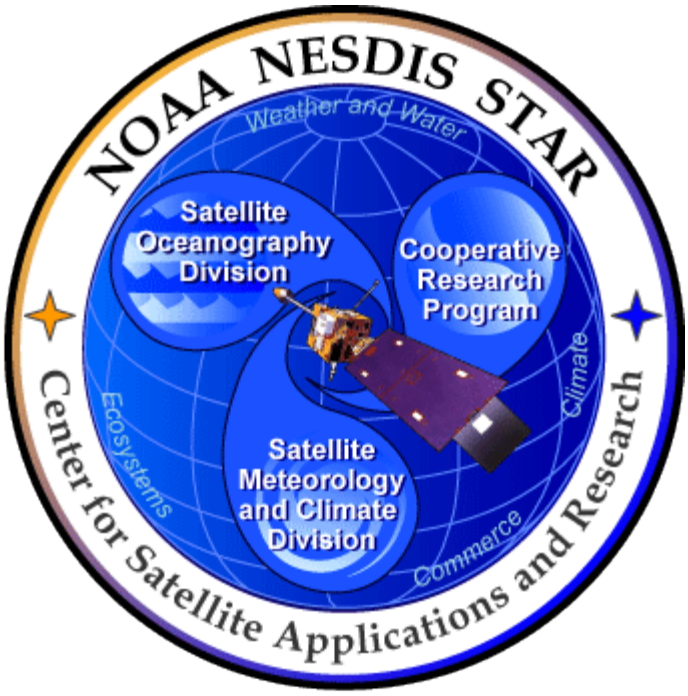

NOAA NESDIS
CENTER for SATELLITE APPLICATIONS and RESEARCH

ALGORITHM THEORETICAL BASIS DOCUMENT

Ice Surface Temperature, Ice Concentration, and Ice Cover

Yinghui Liu, UW/CIMSS

Jeffrey R. Key, NOAA/NESDIS/STAR

Version 1.0

December 17, 2015

TABLE OF CONTENTS

LIST OF FIGURES

LIST OF TABLES

LIST OF ACRONYMS

ABI: Advanced Baseline Imager
AIT: Algorithm Integration Team
AITA: AIT Algorithm
AMSR2: Advanced Microwave Scanning Radiometer 2
AMSR-E: Advanced Microwave Scanning Radiometer - Earth Observing System
ATBD: Algorithm Theoretical Basis Document
AWG: Algorithm Working Group
CIMSS: Cooperative Institute for Meteorological Satellite Studies
DMSP: Defense Meteorological Satellite
EASE-Grid: Equal-Area Earth Grid
FOV: Field of View
GOES-R: Geostationary Operational Environmental Satellite R series
IST: Ice Surface Temperature
JPSS: Joint Polar Satellite System
MODIS: Moderate Resolution Imaging Spectroradiometer
MRD: Mission Requirements Document
MS2GT: MODIS Swath-to-Grid Toolbox
MSG: Meteosat Second Generation
NASA: National Aeronautics and Space Administration
NDSI: Normalized Difference Snow Index
NOAA: National Oceanic and Atmospheric Administration
OLI: Operational Land Imager
SEVIRI: Spinning Enhanced Visible and Infrared Imager
S-NPP: Suomi National Polar Orbiting Partnership
SSMIS: Special Sensor Microwave Imager/Sounder
TIRS: Thermal Infrared Sensor
TOA: Top Of the Atmosphere
USGS: U.S. Geological Survey
VIIRS: Visible Infrared Imaging Radiometer Suite

ABSTRACT

The cryosphere exists at all latitudes an in about one hundred countries. It has profound socio-economic value due to its role in water resources and its impact on transportation, fisheries, hunting, herding, and agriculture. It also plays a significant role in climate studies, and is critical for accurate weather forecasts. Among all the properties of the cryosphere, ice cover, ice concentrations, and ice surface temperature are among most important ones. This document provides high level description of the physical basis and technical approach of the algorithms to identify ice cover and estimate ice concentration and ice surface temperature over water surfaces for clear pixels with supplementary information from satellite observations and retrieved products. This algorithm can be applied to but not limited to the Advanced Baseline Imager (ABI) on the Geostationary Operational Environmental Satellite R series (GOES-R) of National Oceanic and Atmospheric Administration (NOAA) geostationary meteorological satellites, and the Visible Infrared Imaging Radiometer Suite (VIIRS) onboard the Suomi National Polar Orbiting Partnership (S-NPP), and the future Joint Polar Satellite System (JPSS). Group threshold methods are applied on observations from visible and infrared bands to identify ice over water surfaces under clear sky conditions; tie-point algorithm is used to determine the representative reflectance/temperature of 100% ice covered surface, which is in turn applied to estimate the ice concentration. The algorithm is tested extensively using other satellite observations as proxy data of GOES-R ABI, and observations from S-NPP. Validations show that the results meet the requirements of product measurement accuracy and precision.

1 Introduction

1.1 Purpose of This Document

The ice cover and concentration algorithm theoretical basis document (ATBD) provides a high level description of the physical basis and technical approach for the identification of ice cover and estimation of ice concentration and ice surface temperature (IST) over water surfaces for clear pixels with supplementary information from observations and products. This algorithm can be applied to but not limited to the Advanced Baseline Imager (ABI) on the Geostationary Operational Environmental Satellite R series (GOES-R) of National Oceanic and Atmospheric Administration (NOAA) geostationary meteorological satellites, and the Visible Infrared Imaging Radiometer Suite (VIIRS) onboard the Suomi National Polar Orbiting Partnership (S-NPP), and the future Joint Polar Satellite System (JPSS). This algorithm is designed to identify ice over water surfaces including frozen inland lakes and rivers, and oceans, and to provide estimation of ice concentration, fraction in tenths of the sea or lake surface covered by ice, and IST for those ice covered pixels. No land ice applications are included. Output of this algorithm is available to other algorithms, which require knowledge of the ice information. The ice information is also important for planning commercial transportation, short-term weather forecasting, water management, and damage control. Long-term records of ice cover and concentration data are valuable for climate change studies.

1.2 Who Should Use This Document

Intended users of this document are those interested in understanding the physical basis and technical approach of the algorithm, and applying the output of this algorithm for a particular purpose. This document also provides information useful to anyone to implement, maintain and improve the original algorithm.

1.3 Inside Each Section

This document is broken down into the following main sections.

- **System Overview**: Provides relevant details of the ABI, and a brief description of the products to be generated by this algorithm.

- **Algorithm Description**: Provides the detailed description of the algorithm including its physical basis, technical approach, and required input, and output.

- **Assumptions and Limitations**: Provides an overview of the assumptions, limitations of current approach.

1.4 Related Documents

This ATBD extends the related GOES-R ATBDs by adding information specific to VIIRS.

1.5 Revision History

Version 1.0 of this document was created by Yinghui Liu of Cooperative Institute for Meteorological Satellite Studies (CIMSS), University of Wisconsin-Madison, and Jeff Key of NOAA/NESDIS/STAR. It is intended to accompany the delivery of the version 1 algorithms to the GOES-R Algorithm Working Group (AWG) Algorithm Integration Team (AIT).

2 Observing System Overview

As emphasized in the abstract, this algorithm can be applied to multiple satellite platforms. Among those platforms, there are ABI on GOES-R, and VIIRS on S-NPP and JPSS. This section will describe instrument characteristics of ABI and VIIRS, and the products generated this algorithm.

2.1 Instrument Characteristics

The ABI onboard the future GOES-R has a wide range of applications in weather, oceanographic, climate, and environmental studies. ABI has 16 spectral bands (Table 1), with 2 visible bands, 5 near-infrared bands, and 9 infrared bands. The spatial resolution of ABI will be nominally 2 km for the infrared bands, 1 km for 0.47, 0.86, and 1.61 μm bands, and 0.5 km for the 0.64 μm visible band. ABI will scan the full disk every 15 minutes, plus continental United States 3 times, plus a selectable 1000 km × 1000 km area every 30 s. ABI can also be programmed to scan the full disk every 5 minutes. Compared to the current GOES imager, ABI offers more spectral bands and better spatial resolution. Especially, the newly added bands at 1.61 μm, and higher spatial resolution at 0.64 μm allows for a better detection and monitoring of surface snow and ice (Schmit et al. 2005).

Table 1. *Summary of the Current ABI Band Numbers and Wavelengths.*

Band Number	***Wavelength (μm)***	***Subsatellite Field of View (km)***	***Direct Use in AITA***
1	0.47	1	No
2	0.64	0.5	Yes
3	0.86	1	Yes
4	1.38	2	No
5	1.61	1	Yes
6	2.26	2	No
7	3.9	2	No
8	6.15	2	No
9	7.0	2	No
10	7.4	2	No
11	8.5	2	No
12	9.7	2	No
13	10.35	2	No
14	11.2	2	Yes
15	12.3	2	Yes
16	13.3	2	No

The VIIRS onboard the S-NPP and future JPSS satellites has 22 spectral bands covering wavelengths from 0.4 to 11.8 μm (Table 2). The S-NPP was launched on October 28 2011. Among the 22 bands, there are 5 high resolution imagery bands (I-bands, 375 m spatial

resolution at nadir), 16 moderate resolution bands (M-bands, 750 m spatial resolution at nadir), and one Day/Night Band (DNB, 750 m spatial resolution). The VIIRS swath width is 3000 km.

Table 2. *Summary of the VIIRS Band Numbers and Wavelengths.*

Band Number	***Wavelength (μm)***	***Subsatellite Field of View (km)***	***Direct Use in AITA***
M1	0.411	0.750	No
M2	0.444	0.750	No
M3	0.486	0.750	No
M4	0.551	0.750	No
I1	0.639	0.375	No
M5	0.672	0.750	Yes
M6	0.745	0.750	No
I2	0.862	0.375	No
M7	0.862	0.750	Yes
M8	1.238	0.750	No
M9	1.375	0.750	No
I3	1.602	0.375	No
M10	1.602	0.750	Yes
M11	2.257	0.750	No
I4	3.753	0.375	No
M12	3.697	0.750	No
M13	4.067	0.750	No
M14	8.578	0.750	No
M15	10.729	0.750	Yes
I5	11.469	0.375	No
M16	11.845	0.750	Yes
DNB	0.7	0.750	No

Inputs of this algorithm include observations at 0.64 μm, 0.86 μm, 1.6 μm, and split window channels at 10 and 11 μm, which are band 2, 3, 5, 14, and 15 for ABI, and M5, M7, M10, M15, and M16 for VIIRS.

2.2 Products Generated

The ice cover, ice concentration, and IST algorithm is responsible for identification of all pixels covered with ice over water surfaces under clear conditions, and estimation of ice concentration and IST. No land ice applications are included.

Ice cover reports the location of ice over frozen inland lakes, rivers, and open waters, and ice concentration reports the fraction (in tenths) of the sea or lake surface covered by ice, and IST reports the temperature of those ice-covered pixels. Total concentration includes all ice types that are present.

The required product Function and Performance Specification (F&PS) for ice cover and ice concentration of GOESE-R ABI are listed in Table 3 and 4 respectively.

Table 3. *Product Function and Performance Specification for ice cover from GOES-R ABI.*

Name	Ice Cover
User and Priority	GOES-R
Geographic Coverage (G, H, C, M)	FD
Vertical Resolution	N/A
Horizontal Resolution	2km
Mapping Accuracy	1km
Measurement Range	Binary yes/no detection
Measurement Accuracy	85% correct detection
Product Refresh Rate/Coverage Time	180 min
Vendor Allocated Ground	77,756 sec
Product Measurement Precision	N/A

Table 4. *Product Function and Performance Specification for ice concentration from GOES-R ABI.*

Name	Sea & Lake Ice Concentration	Sea & Lake Ice Concentration
User and Priority	GOES-R	GOES-R
Geographic Coverage (G, H, C, M)	C: Regional and Great Lakes and US costal waters containing sea ice hazards to navigation	FD: Sea ice covered waters in N & S Hemisphere
Vertical Resolution	Ice Surface	Ice Surface
Horizontal Resolution	3 km	10 km
Mapping Accuracy	<= 1.5 km	<= 5 km
Measurement Range	Ice concentration 1/10 to 10/10	Ice concentration 1/10 to 10/10
Measurement Accuracy	10%	10%
Product Refresh Rate/Coverage Time	180 min	6 hr
Vendor Allocated Ground	3236 sec	9716 sec
Product Measurement Precision	30%	30%

Table 5. *Product Function and Performance Specification for ice concentration from S-NPP and JPSS VIIRS.*

Name	User & Priority	Geographic Coverage	Vertical Res.	Horiz. R...	Mapping A...	Msmnt. Range	Msmnt. Accuracy	Product Refresh Rate/Coverage Time	Vendor Allocated Ground Latency	Product Measurement Precision	Temporal Coverage Qualifiers	Product Extent Qualifier	Cloud Cover Conditions Qualifier	Product Statistics Qualifier
Ice Concentration	JPSS VIIRS	All ice-covered regions of the global ocean	Ice Surface	1 km	1 km	Ice concentration – 0/10 to 10/10	Ice concentration – 10%	At least 90% coverage of the globe every 24 hours	3236 sec	30%	All conditions	Quantitative under all conditions	Clear conditions associated with threshold accuracy	Over specified geographic area

Table 6. *Product Function and Performance Specification for ice cover from S-NPP and JPSS VIIRS.*

Name	User & Priority	Geographic Coverage	Vertical Res.	Horiz. Res.	Mapping Accuracy	Msmnt. Range	Msmnt. Accuracy	Product Refresh Rate/Coverage Time	Vendor Allocated Ground Latency	Product Measurement Precision	Temporal Coverage Qualifiers	Product Extent Qualifier	Cloud Cover Conditions Qualifier	Product Statistics Qualifier
Ice: Cover (mask)	JPSS VIIRS	FD	N/A	1 km	1 km	From the 100% ice concentration at the land edge to the less then 15% ice concentration that is	1 km	180 min	90% coverage of the globe every 24 hours	80% probability of correct typing	All condition	All condition	Clear conditions associated with threshold accuracy	Over specified geographic area

						the ice extent								

Table 7. *Product Function and Performance Specification for ice surface temperautre from S-NPP and JPSS VIIRS.*

Name	User & Priority	Geographic Coverage (G, H, C, M)	Vertical Res.	Horiz. Res.	Mapping Accuracy	Msmnt. Range	Msmnt. Accuracy	Product Refresh Rate/Coverage Time	Vendor Allocated Ground Latency	Product Measurement Precision	Temporal Coverage Qualifiers	Product Extent Qualifier	Cloud Cover Conditions Qualifier	Product Statistics Qualifier
Ice Surface Temperature	JPSS VIIRS	All ice-covered regions of the global ocean	Ice Surface	1.6 km	1.6 km	213 – 275 K	1 K	At least 90% coverage of the globe every 24 hours	3236 sec	1 K	All conditions	Quantitative under all conditions	Clear conditions associated with threshold accuracy	Over specified geographic area

The ice cover will be produced for each pixel over water surface, and ice concentration and IST will be calculated for each pixel covered with ice. Both products are for pixels under clear-sky condition only. This algorithm relies on the accuracy of other dependent products including cloud mask, land/water mask, and etc. Details of the required input parameters and current validations are presented in the following sections. Algorithm sensitivity study will be reported in the upcoming next version.

3 Algorithm Description

Complete description of the algorithm is presented at the current level of maturity. The algorithm will be updated with each revision.

3.1 Algorithm Overview

This automated algorithm detects ice cover and retrieves ice concentration. Ice cover is first determined by a group-criteria technique. Then ice concentration is retrieved based on the determined normalized reflectance/BT of pure ice and pure water through application of a tie point algorithm. Ice cover is further refined based on the retrieved ice concentration.

Pros: This automated algorithm is designed on solid physical foundation, and is capable of identifying ice cover and retrieving concentration for both day and nighttime. It runs automatically, and can be employed globally.

Cons: The accuracy of this algorithm depends on the quality of the cloud mask, and no retrieval can be carried out for cloudy pixels.

3.2 Processing Outline

The processing outline of this algorithm is summarized in Figure 1.

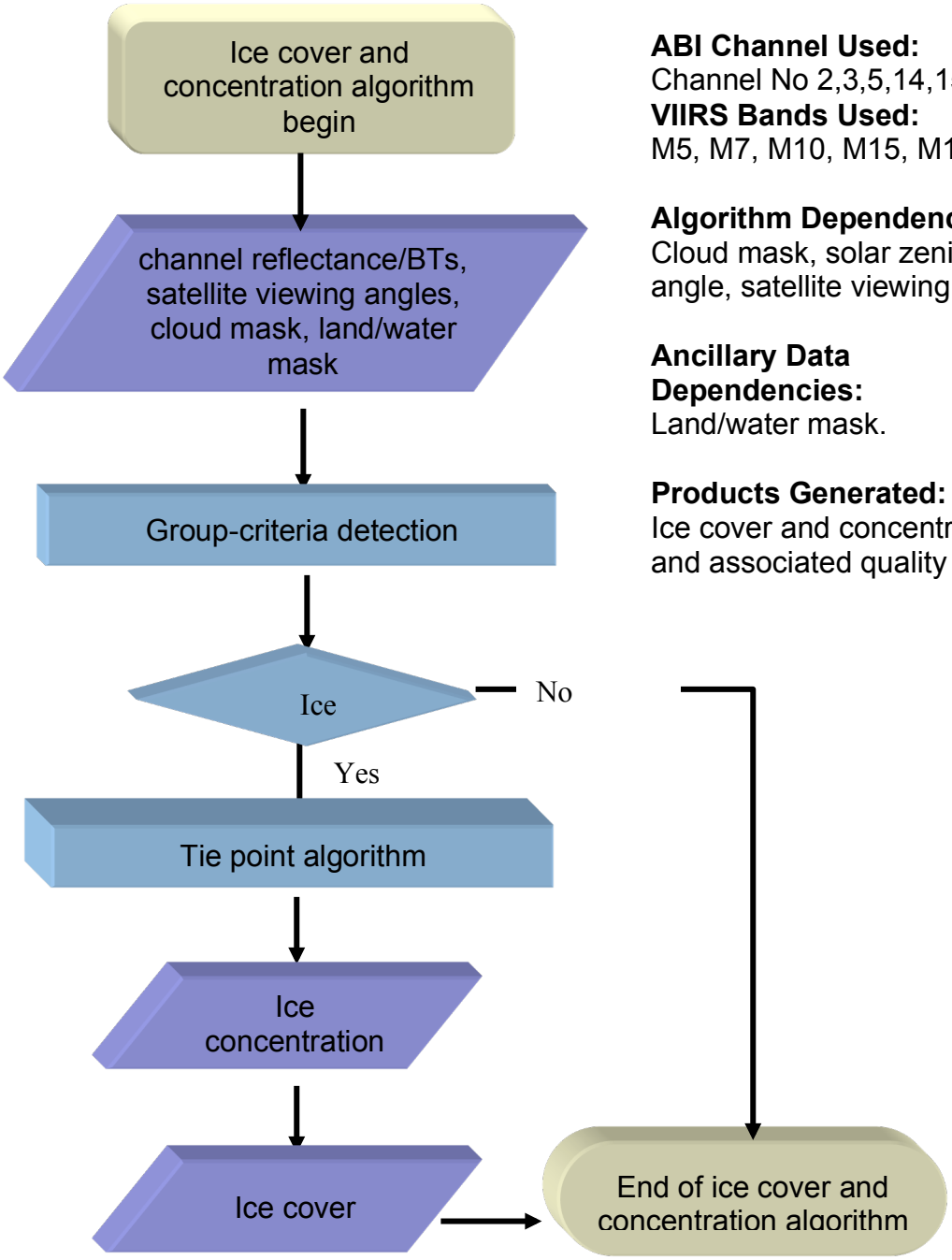

Figure 1. *High Level Flowchart of the ice cover and concentration algorithm illustrates the Main Processing Sections.*

3.3 Algorithm Input

This section describes the input of this ice cover and concentration algorithm.

3.3.1 Primary Sensor Data

The list below contains the primary parameter data used in this algorithm. Primary parameter data represents information that is derived mainly from the ABI observations and geo-location information. All the input data are used in its original spatial resolution. The primary sensor data are:

- Reflectance in bands 0.46 um, 0.55 um, 0.64 um, 0.86 um, and 1.6 um, which are VIIRS Mbands 3, 4, 5, 7, and 10
- Brightness Temperatures in bands 11 um, and 12 um, which are VIIRS Mbands 15 and 16
- Latitude
- Latitude
- Longitude
- Sensor viewing zenith angle
- Solar zenith angle
- Scattering angle

The pixel level spatial resolution of ABI band 2, 3, 5, 14, and 15 are 0.5 km, 1 km, 1 km, 2 km, and 2 km at sub-satellite Field Of View (FOV), and 0.750 km sub-satellite FOVfor VIIRS M5, M7, M10, M15, and M16 bands . The required horizontal resolution of the ABI outputs are at 2 km for ice cover, and 3 km, and 10 km for regional and global ice concentration retrievals, and 1km for VIIRS sea ice cover and concentration, and 1.6 km for IST. This algorithm in this version is capable of producing outputs with the spatial resolution at the lowest ABI pixel level spatial resolution (2 km), and 0.750 km spatial resolution for VIIRS. Both the VIIRS and ABI cloud mask are 4-level cloud mask, clear, probably clear, probably cloudy, and cloudy. Cloud mask input for this algorithm includes two categories: clear (clear and probably clear in cloud mask), and cloudy (cloudy and probably cloudy). The cloud shadow, and sun glint determination comes from VIIRS and ABI cloud mask.

3.3.2 Ancillary Data

Ancillary data are data that requires information not included in the satellite observations, derived products, or geo-location data. The following ancillary data are required:

- Land mask

These data come from the geolocation data. There are total four values in the current land mask as input. Value 0 represents the ocean water surface, including shallow ocean (ocean is less than 5 kilometers from the coast or with depth less than 50 meters), moderate or continental ocean

(ocean is more than 5 kilometers from the coast and with depth between 50 and 500 meters), and deep ocean (depth larger than 500 meters) as categorized in MODIS geolocation data; value 1 stands for in-land water surface, including shallow inland water (inland water less than 5 kilometer from shoreline or depth less than 50 meters), ephemeral water, and deep inland water (inland water more than 5 kilometer from shoreline and depth more than 50 meters); value 2 means land surface, including land, ocean coastlines, and lake shorelines; value 3 includes all other pixels, including bow-tie delete pixels.

3.3.3 Derived Data

The following derived data are required by the algorithm:

- Cloud Mask and sun glint information from Cloud Mask
- Shadow Mask from Cloud height
- Derived surface skin temperature by this algorithm

3.4 Theoretical Description

Sea and lake ice influences the surface radiation budget, and affects energy and moisture exchange between the atmosphere and the underlying water. It is one of the key factors to consider in the atmospheric circulation, numerical weather forecasting, and climate models. Ice cover is also important for planning commercial transport. Ice cover and concentration are among the most important indices in studying climate change. Accurate retrievals of ice cover and concentration are of high importance both to the scientific communities and to the public.

In the following sections, the physical background and technical approaches of the processes in this algorithm is described.

3.4.1 Physics of the Problem

3.4.1.1 Ice and snow reflectance

Ice surface reflectance depends strongly on its internal structure, such as brine pockets, air bubbles of the near surface layers. These internal structures change with season, state of the near surface layers, and age of ice, which results in different ice types. Reflectance of ice surface is different from that of snow surface. Ice consists mainly of sheets, while snow consists of grains. Absorption and scattering in the snow and ice surface are determined by their internal inhomogeneities (Grenfell and Maykut, 1977). Snow reflectance shows very high values at visible channels, but low values at short-wavelength channels longer than 1.4 microns (Bolsenga 1983), due to the much stronger absorption and much less back scattering at those infrared channels. This feature is shared by snow-covered ice and many ice types. Most of the ice

surfaces show higher reflectance at visible and near infrared channels than water surface, which can be used to detect ice cover. Other substances do not have this unique spectral signature of snow and ice. Clouds have high reflectance at both visible and near infrared channels. Water surface is dark at all wavelengths (Riggs et al. 1999). However, some ice types, such as clear lake ice, grease ice, can be difficult to detect for very low contrast with open water.

3.4.1.2 Ice surface temperature

Ice surface temperature is retrieved using brightness temperatures at split window channels at 10 and 11 μm, which are ABI band 14 and 15, and M15 and M16 for VIIRS, and satellite sensor scan angle derived from sensor zenith angle. The retrieval algorithm is from the work of Key et al. (1997). To retrieve ice/snow surface skin temperature (IST), the following equation is used.

$$Ts = a + bT11 + cT12 + d\,[(T11-T12)(\sec\theta-1)] \qquad (1)$$

where Ts is the estimated surface skin temperature (Unit: Kelvin), T11 and T12 are the brightness temperatures (K) at 11 um and 12 um bands, and θ is the sensor scan angle. Coefficients a, b, c, and d (Table 4) are derived for the following temperature ranges: T11 < 240K, 240K < T11 < 260K, T11 > 260K. The coefficients are based on modeled radiances in the 11 and 12 um bands using Arctic and Antarctic temperature and humidity profiles, and angular emissivity models for snow. The equations do not include a bias term to account for differences between modeled and actual radiances. This has not been necessary for NOAA-14, which as validated extensively with surface data from the SHEBA experiment, and for MODIS. This bias term is not included in the current S-NPP VIIRS IST, however it will be considered for future JPSS VIIRS based on further validation. Though the bias term is not expected for ABI, conclusion needs be drawn based on validations of retrieved ice surface temperature using ABI with in situ observations after launch of GOES-R. See Key et al. (1997) for additional details. The coefficients for the current S-NPP VIIRS is included in Table 8. The coefficients were updated for Moderate Resolution Imaging Spectroradiometer (MODIS) onboard the Terra and Aqua satellites (see the values of these coefficients for MODIS in Table 9), and for Spinning Enhanced Visible and Infrared Imager (SEVIRI) onboard the Meteosat Second Generation (MSG) satellites, and will be updated for GOES-R ABI once the spectral response functions of ABI bands are determined. In equation (1), the sensor scan angle is derived from the sensor zenith angel using the equation (2).

$$\theta = \arcsin\left(\sin(\lambda) \times R_e / \left(R_e + A_{sat} \right) \right) \qquad (2)$$

where λ is the sensor zenith angle, R_e is the equatorial radius of the Earth, A_{sat} is the nominal altitude of the satellite.

This method is specifically designed for retrievals over ice/snow surface, which is not provided from the land team.

Table 8. *Values of coefficients a, b, c, and d in equation (1) for S-NPP VIIRS*

Temperature Range	a	b	c	d

Arctic	< 240 K	-7.560993	1.031344	1.248151	-0.406514
	240 – 260 K	-8.918637	1.036658	0.514256	2.111948
	> 260 K	-6.872886	1.028288	1.019783	2.340682
Antarctic	< 240 K	-2.398863	1.010777	-0.225380	0.457090
	240 – 260 K	-9.688947	1.040270	-0.463295	2.862228
	> 260 K	-9.016985	1.036905	0.330130	2.595204

Table 9. *Values of coefficients a, b, c, and d in equation (1) for MODIS*

Temperature Range		a	b	c	d
Antarctic	< 240 K	-0.159480	0.999926	1.390388	-0.413575
	240 – 260 K	-3.329456	1.012946	1.214573	0.131017
	> 260 K	-5.207360	1.019429	1.510250	0.260355
Arctic	< 240 K	-0.159480	0.999926	1.390388	-0.413575
	240 – 260 K	-3.329456	1.012946	1.214573	0.131017
	> 260 K	-5.207360	1.019429	1.510250	0.260355

3.4.2 Mathematical Description

3.4.2.1 Ice detection

Ice cover is detected at the pixel level over water surface under clear conditions. Clear condition is determined from the input cloud mask.

Snow covered ice show high reflectance in the visible channels, and very low reflectance in short-wavelength infrared channels. Many ice types also have this characteristic, and most ice types have higher reflectance than open water, which typically has a very low reflectance.

Traditionally, Normalized Difference Snow Index (NDSI) is used to detect snow and ice. NDSI is defined as

$$NDSI = (R_1 - R_2)/(R_1 + R_2) \qquad (3)$$

where R_1 is often the reflectance in visible channel, (e.g. 0.55 μm for MODIS), R_2 is the reflectance in short-wavelength infrared channel (e.g. 1.6 or 2.1 μm for MODIS). Ice is identified when NDSI is larger than a preset threshold. In this algorithm, 0.86 μm and 1.6 μm are selected for R_1 and R_2, band M7 and M10 for VIIRS, and band 3 and 5 for ABI. Both bands have the same spatial resolution for ABI (1km at sub-satellite Field of View (FOV)) and VIIRS. Furthermore, one advantage of 0.865 μm over 0.55 μm to calculate NDSI is that NDSI calculated using 0.55 μm reflectance is higher than preset threshold over water surfaces in some cases, while NDSI from 0.865 μm is mostly lower than the preset threshold.

Ice cover has colder surface temperature than open water. And water with higher salinity usually has lower melting temperature.

In daytime (solar zenith angle lower than 85 degree), a pixel is identified as possible ice covered if the NDSI value is larger than a threshold, 0.45 for VIIRS and 0.6 for ABI, the reflectance at 0.865μm, VIIRS band M7 and ABI band 3, higher than 0.08 (Hall et al. 2001, 2006), and surface temperature lower than preset thresholds (275 K over both fresh water salty and ocean water). The reason not to use the melting temperature, 27.15 K for fresh water and 271.5 K for salty ocean water, is that some ice-covered pixels with melting water have surface temperature have higher values.

During nighttime (solar zenith angle higher than or equal to 85 degree), a pixel is identified as possible ice covered if surface temperature is lower than 275.0 K over lake or river (fresh water), and over ocean (salty) water.

3.4.2.2 Ice concentration from tie points algorithm

Ice characteristics change temporally and spatially. Different ice types can appear simultaneously in a large field of view, and change over time. Under certain conditions that a single ice type appears in a search window with certain shape (a square or a circle) and size, surface reflectance or temperature of the pure ice is homogeneous, while distinct from open water. Changes in surface reflectance/temperature at pixel level are mainly due to changing ice concentrations, fraction of the surface covered by ice. Theoretically, the reflectance and temperature of pure ice and open water can be derived from a tie point method applied in a search window, if 100% ice covered pixels are the majority of all ice covered pixels in each search window (Figure 2a, 2b).

Then, ice concentration for a pixel (F_p) inside the search window can be calculated by

$$F_p = (B_p - B_{water}) / (B_{ice} - B_{water}) \qquad (4)$$

where B_{water} is the reflectance/temperature of pure water pixels, B_{ice} is the reflectance/temperature of pure ice pixels; B_p is the observed reflectance/temperature of the pixel, of which ice concentration will be calculated. In this algorithm, reflectance at 0.64 μm, VIIRS band M5 and ABI band 2, is selected in daytime, and surface skin temperature is selected at nighttime. Surface skin temperature can also be used in daytime. Whether the final ice concentration in daytime uses only the retrievals from reflectance, or only the retrievals from surface skin temperature, or the optimal combination of both retrievals need further investigation. In the current version of this algorithm, ice concentration from the reflectance is used in the daytime. For VIIRS, the spatial resolution is 0.750 km; for ABI, the spatial resolution is 0.5 km at 0.64 μm band, and 2.0 km for surface temperature at sub-satellite FOV.

Determination of the reflectance/temperature of pure ice pixels is the key to calculate the ice concentration. In a square search window with a size of 50 pixel × 50 pixel, ice reflectance/temperature probability density function (PDF) is calculated using all the possible ice covered pixels detected in the first step described in section 3.4.2.1. The size of the search

window is determined as an algorithm input. This PDF is presented as a histogram bins. For reflectance, the minimum bin value is 0., with bin width 0.02, total bin number 121 to be consistent with temperature. For temperature, the minimum bin value is 215 K, with bin width 0.5 K, total bin number 121. The histogram bins are then smoothed by a running boxcar filter with the width of 5 bins, in which a sliding integral is calculated over the original PDF. A new smoothed PDF is derived as the result. The ice reflectance/temperature tie point is chosen as the reflectance/temperature with the maximum probability density in the smoothed PDF, i.e. the maximum sliding integral. The tie point reflectance of open water is parameterized as a function of solar zenith angle, with 0.05 for solar zenith angle less than 65 degree and 0.07 for solar zenith angle larger or equal to 65 degree. The tie point surface temperature of open water changes with the water salinity, 275.0 K for fresh water and salty water. The tie point algorithm described above is adapted from the similar algorithm by Appel and Kenneth (2002). The reason that the location of the max PDF point is selected as the tie point of pure ice is that ice with 100% ice concentration is assumed to be majority in a search window, and the ice characteristics are homogeneous in the search window.

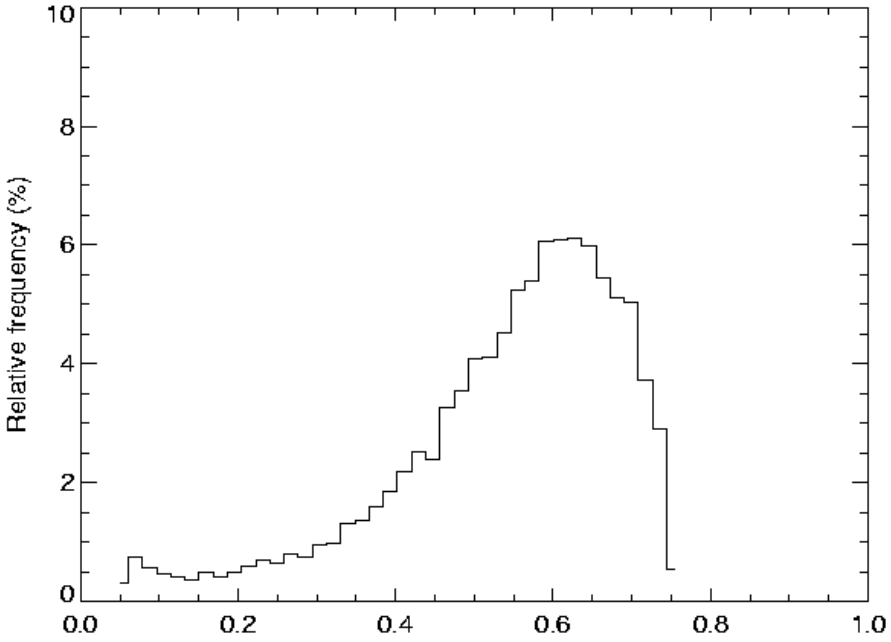

Figure 2a. *Reflectance probability density distribution at 0.64 μm for ice cover over Lake Erie on Feb 24, 2008.*

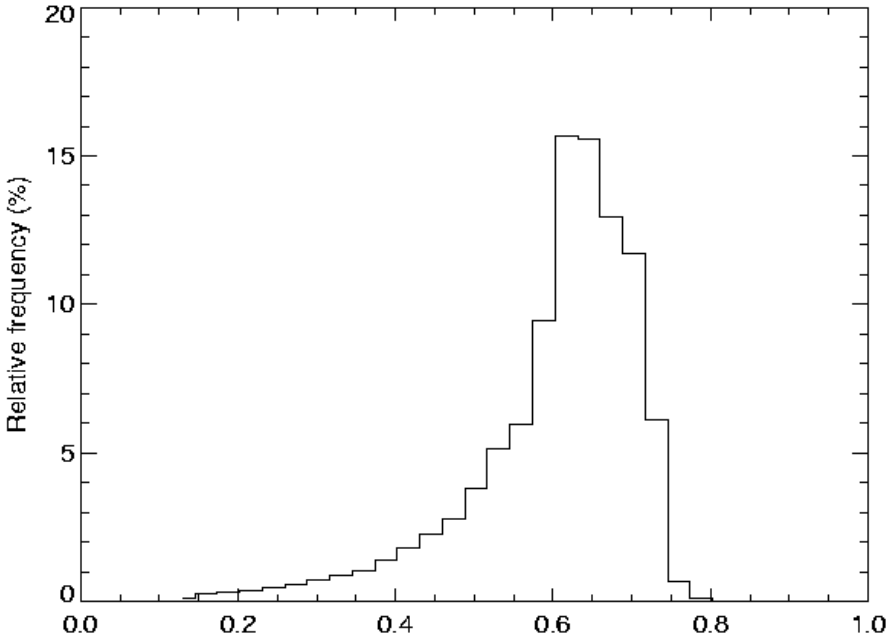

Figure 2b. *Reflectance probability density distribution at 0.64 μm for ice cover over Barents and Kara Seas on Mar 31, 2008.*

3.4.2.3 Ice cover

Ice cover is first determined after ice detection tests, and refined with retrieved ice concentration. As the first step, pixels with ice detected at daytime are assigned value 1, and value 2 at nighttime when only surface skin temperature test is used. Pixels with water covered are assigned value 3. After that ice concentration is retrieved, ice pixels determined in the first step are assigned value -2 (water surface) if retrieved ice concentration is less 15%.

3.4.3 Algorithm Output

The outputs of this algorithm are:

- Ice Concentration
- Ice Cover
- Ice Surface Temperature
- Quality control (QC) flags
- Metadata

These are described in Tables 10 and 11.

Table 10. *Output and additional output parameters and their definitions.*

Definition	**Description**	**Unit**
Ice concentration	The fraction (in tenths or percentage) of the sea or lake surface covered by ice	Unitless
Ice cover	A pixel is ice covered or not. Value 1: ice detected using daytime tests 2: ice detected using nighttime tests 0: cloud -1: land -2: water surface -3: non-retrievable due to sunglint, cloud shadow, and missing pixels	Unitless
Ice surface temperature (additional)	Skin temperature at ice surface	Kelvin

Table 11. *Ice Cover and Concentration Quality Information (4 bytes)*

Byte	Bit	Quality Flag Name	Description	Meaning
1	0	QC_output	Output product quality	00 - normal 01 - uncertain 10 – non-retrievable 11 – bad data
	1			
	2	QC_INPUT_CLD	Input cloud mask	00 - clear 01 - probably clear 10 -probably cloudy 11-cloudy
	3			
	4	QC_INPUT_DAY	Day/Night	0-Day 1-Night
	5	QC_INPUT_SUNGLINT	Sunglint or not	0-Yes 1-No
	6	QC_INPUT_CLDSHADOW	Cloud shadow or not	0-Yes 1-No
	7	empty		
2	0	QC_INPUT_SOLZEN	Valid solar zenith angle (0-180 degree)	0-Yes 1-No
	1	QC_INPUT_SATZEN	Valid satellite zenith angle (0-180 degree)	0-Yes 1-No
	2	QC_INPUT_REFL	Valid reflectance at 0.47 μm (0.0-1.0)	0-Yes 1-No
	3		Valid reflectance at 0.64 μm (0.0-1.0)	0-Yes 1-No
	4		Valid reflectance at 0.86 μm (0.0-1.0)	0-Yes 1-No
	5		Valid reflectance at 1.6 μm (0.0-1.0)	0-Yes 1-No
	6	QC_INPUT_THERMAL	Valid brightness temperature at 10 μm (100-390 k)	0-Yes 1-No

	7		Valid brightness temperature at 11 μm (100-390 k)	0-Yes 1-No
3	0	QC_INPUT_SURFACE	Surface type flag	00 - in-land water 01 - sea water 10- land 11 - others
	1			
	2	QC_TEST_REFL	Success of reflectance test in ice cover detection	0-Yes 1-No
	3	QC_TEST_NDSI	Success of NDSI test in ice cover detection	0-Yes 1-No
	4	QC_TEST_SKINTEMP	Success of skin temperature test in ice cover detection	0-Yes 1-No
	5	QC_TIE_REFL	Success of visible band tie-point algorithm	0-Yes 1-No
	6	QC_TIE_SKINTEMP	Success of skin temperature tie-point algorithm	0-Yes 1-No
	7	empty		
4	0	QC_READ_INPUT	Success in reading input	0-Yes 1-No
	1			
	2			
	3			
	4			
	5			
	6			
	7			

Metadata are also included in the final product. The metadata include the common metadata for all data products and specific metadata for ice cover and concentration product.

Common metadata for all data products:

- DateTime (swath beginning and swath end)
- Bounding Box
  - Product resolution (nominal and/or at nadir)
  - Number of rows, and number of columns
  - Bytes per pixel
  - Data type
  - Byte order information
  - Location of box relative to nadir (pixel space)
- Product Name
- Product units
- Ancillary data to produce product (including product precedence and interval between datasets is applicable)
  - Version Number
  - Origin
  - Name

- Satellite
- Instrument
- Altitude
- Nadir pixel in the fixed grid
- Attitude
- Latitude, longitude
- Grid projection
- Type of scan
- Product version number
- Data compression type
- Location of production
- Citations to documents
- Contact information

Ice Cover and Concentration Specific Metadata:

- Number of QA flag values (currently, there are 4: Normal or Optimal; Uncertain or Suboptimal; Non-retrievable; Bad data)
- For each QA flag value, the following information is provided:
  - Definition of QA flag
  - Total pixel numbers with the QA flag
- Total number of pixels with water surface
- Total number of valid ice cover and concentration retrievals (normal+uncertain)
- Total percentage of valid ice cover and concentration retrievals of all pixels with water surface
- Total pixels numbers and percentage of terminator pixels (Non-retrievable and Bad data)
- Pixel number of daytime ice cover and concentration valid retrievals
- Pixel number of nighttime ice cover and concentration valid retrievals
- Mean, Min, Max, and standard deviation of valid ice concentration retrievals
- Pixel size of search window to determine tie-point.

4 Validations with test datasets and S-NPP VIIRS

4.1 Simulated Input Data Sets

Proxy data of GOES-R ABI used to test this algorithm included observations from MODIS, Spinning Enhanced Visible & InfraRed Imager (SEVIRI) onboard of the MSG (Meteosat Second Generation) satellites. The channels in the proxy data associated with GOES-R ABI are listed in Table 7. Validations were performed by comparison to passive microwave ice cover and concentration product from Advanced Microwave Scanning Radiometer - Earth Observing System (AMSR-E) observations, comparison with true-color satellite images, and comparison with ice cover and ice concentration of ice chart from National Ice Center and Environment Canada are detailed in the following subsections. Our testing and validations include both sea and lake ice.

Table 12. *Channels in the proxy data associated with GOES-R ABI.*

ABI Band Number	***ABI Wavelength (μm)***	***MODIS band v (Wavelength μm)***	***SEVIRI band (Wavelength μm)***
2	0.64	1 (0.64)	1 (0.635)
3	0.86	2 (0.86)	2 (0.81)
5	1.61	6 (1.6)	3 (1.64)
14	11.2	31 (11)	9 (10.80)
15	12.3	32 (12)	10 (12.0)

4.1.1 MODIS Data

MODIS (Moderate Resolution Imaging Spectroradiometer) is a key instrument aboard the Terra (*EOS AM, refer to http://terra.nasa.gov/*) and Aqua (*EOS PM, refer to http://aqua.nasa.gov/*) satellites. Terra's orbit around the Earth is timed so that it passes from north to south across the equator in the morning, while Aqua passes south to north over the equator in the afternoon. The MODIS instrument has a viewing swath width of 2,330 km and views the entire surface of the Earth every one to two days. Its detectors measure 36 spectral bands between 0.405 and 14.385 μm, and it acquires data at three spatial resolutions -- 250m, 500m, and 1,000m.

Figure 3 shows an example of sea ice concentration (SIC) retrievals from MODIS data as the proxy of GOES-R ABI. Left panel in Figure 3 shows the ice concentration retrieval based on MODIS retrieved ice surface skin temperature, and right panel shows the ice concentration retrieval based on MODIS visible band reflectance at 0.64 μm. Both retrievals show similar results, with high sea ice concentration near the North Pole and lower values near the ice edges. This example shows that this algorithm works for sea ice concentration retrieval using MODIS data.

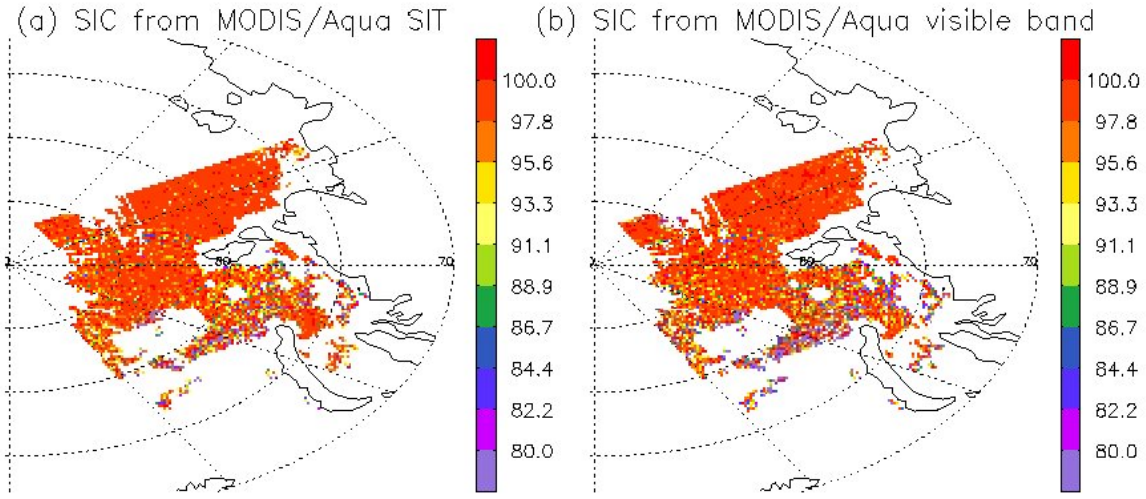

Figure 3. *Sea ice concentration (%) retrieved from (a) MODIS Sea Ice Temperature (SIT), (b) MODIS visible band (0.64 μm) reflectance using tie points algorithm on March 31st 2006.*

Figure 4 shows another example of ice concentration retrievals over the Great Lakes and inland waters from MODIS observations. The retrieved ice concentration agrees well with those observed from the MODIS true color image. This example shows that this algorithm works for lake ice concentration retrieval using MODIS data.

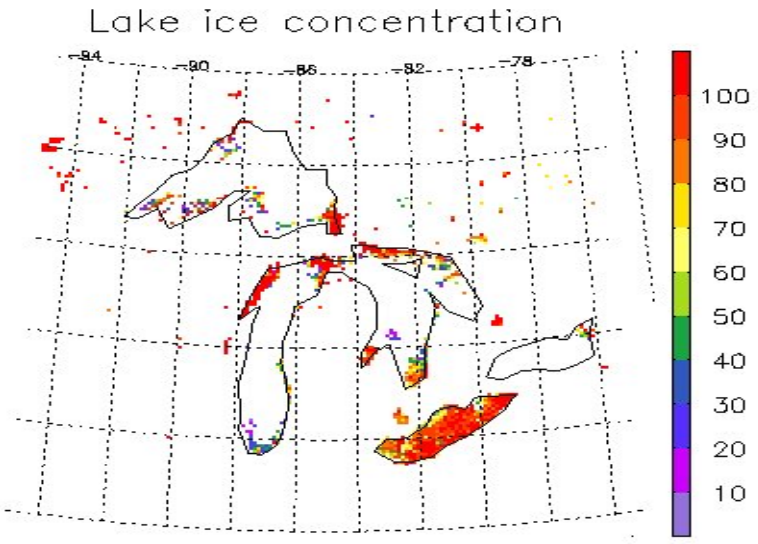

Figure 4. *Lake ice concentration (%) with MODIS Aqua visible band (0.64 μm) data on February 24, 2008.*

4.1.2 SEVIRI Data

SEVIRI is the primary payload of the MSG satellites, which form a joint project between the European Space Agency and Eumetsat, the European Organisation for the Exploitation of Meteorological Satellites since 1977 (*refer to http://www.eumetsat.int/home/Main/Access_to_Data/Meteosat_Image_Services/SP_1123237865326*). SEVIRI measures reflected and emitted radiance in 11 spectral channels located between 0.6 μm and 14 μm with a nominal spatial resolution of 3 km at the sub-satellite point alone with an additional broadband high-resolution visible (0.4-1.1 μm) channel that has a 1 km spatial resolution. The full disc view allows frequent sampling, every 15 minutes, enabling monitoring of rapidly evolving events. The nominal coverage includes the whole of Europe, Africa and locations at which the elevation to the satellite is greater than or equal to 10^{o}.

Figure 5 shows an example of ice concentration retrievals over the Caspian Sea from SEVIRI observations. The left panel shows the retrieval based on SEVIRI retrieved ice surface

temperature, and the right panel shows the ice concentration retrieval based on SEVIRI visible band reflectance at 0.64 μm. Both retrievals show very similar results, with higher ice concentration over the northern part, decreasing southward, and eventually open water. Comparison of the retrieved ice concentration to those observed from satellite true color image show good agreement, which demonstrates that this ice concentration retrieval algorithm works for lake ice concentration retrieval using SEVIRI data.

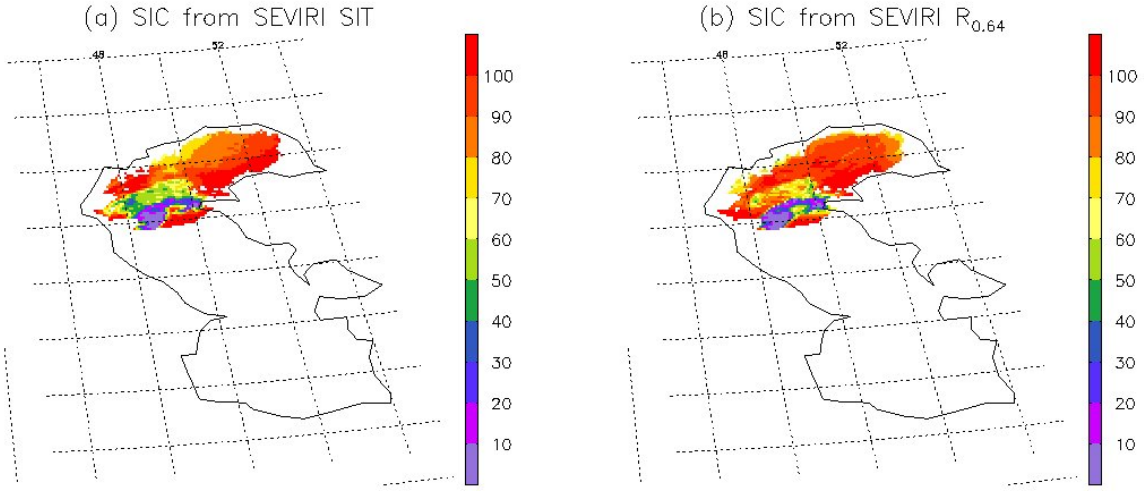

Figure 5. *Lake ice concentration (%)retrieved from (a) SEVIRI Surface Ice Temperature (SIT), (b) SEVIRI visible band reflectance (0.64 μm) on January 27, 2006.*

4.2 Output from Simulated Inputs Data Sets

4.2.1 Precisions and Accuracy Estimates

Product measurement accuracy requirement for ice cover is 85% correction detection. The product measurement accuracy requirement for ice concentration is 10%, with a product measurement precision of 30%. Direct match ups and comparison between satellite retrieved ice cover and concentration and satellite true color images are made to gain qualitative results. Comparison of the retrieved products with ice cover and concentration from microwave observations, and ice chart provides quantitative results, with mean bias, standard deviation, and bias frequency distribution presented.

Routine validations of retrieved ice cover and concentration with those from microwave, and ice chart products will continue. Validations of satellite retrieved ice cover and concentration with those from the Thematic Mapper onboard Landsat 6 and 7 with spatial resolution of 30 meters will be included.

4.2.1.1 Comparison with the AMSR-E product

The AMSR-E instrument onboard Aqua Satellite is a twelve-channel, six-frequency, conically-scanning, passive-microwave radiometer system. It measures horizontally and vertically polarized microwave radiation (brightness temperatures) ranging from 6.9 GHz to 89.0 GHz. Spatial resolution of the individual measurements varies from 5.4 km at 89 GHz to 56 km at 6.9 GHz. The AMSR-E instrument provides measurements of land, oceanic, and atmospheric parameters, including sea ice concentration, snow water equivalent, and etc.

The AMSR-E Level-3 gridded product (AE_SI12) includes sea ice concentration mapped to a polar stereographic grid at 12.5 km spatial resolution. This dataset is used for comparison with the sea ice concentration retrievals using MODIS as proxy data of the GOES-R ABI.

Figure 6 shows an example of comparison of sea ice concentration from AMSR-E product and from MODIS. Both products show similar patterns in the sea ice concentration, high values in the central Arctic and lower value towards to Barents Sea. The MODIS retrievals show more details in the central Arctic in correspondence to leads in the sea ice. The MODIS retrievals also show lower sea ice concentration towards the open water. Although AMSR-E is not ground truth, statistical estimates of difference between these sea ice concentrations might provide helpful information for improvement of the retrieval algorithm. The MODIS sea ice concentrations were averaged for 11x11 pixels (native resolution is 1 km at the sub-satellite point) centered on the AMSR-E footprint (about 12 km nadir). For this specific case, the bias and standard deviation between AMSR-E and MODIS surface skin temperature (reflectance) based sea ice concentration are 2.8% (5.6%), and 4.1% (7.5%).

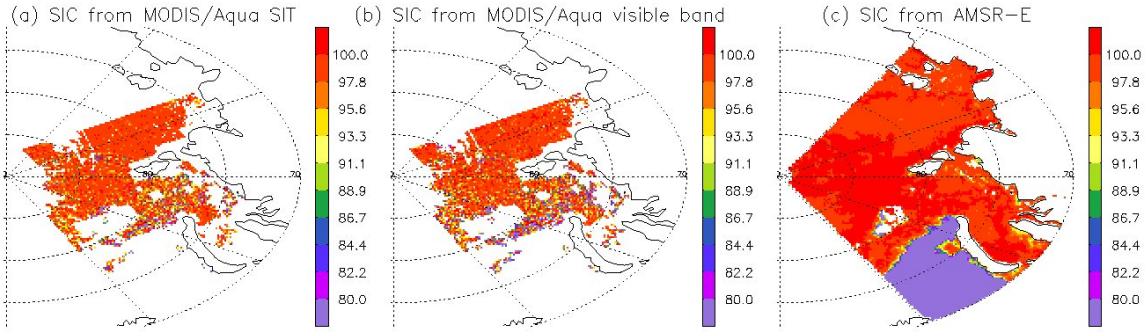

Figure 6. *Sea ice concentration (SIC) (%) retrieved from (a) MODIS Sea Ice Temperature (SIT), (b) MODIS visible band reflectance, and (c) from Advanced Microwave Scanning Radiometer - Earth Observing System (AMSR-E) Level-3 gridded daily mean from NSIDC on March 31, 2006.*

4.2.1.2 Comparison with the satellite true color images

Lake ice concentrations are also compared with the satellite true color images for qualitative purpose. Though these comparisons cannot give quantitative results, it helps to show whether the retrieved ice cover and concentration have reasonable distributions.

Figure 7 gives another example of comparison of MODIS retrieved lake ice concentration with satellite true color image. The lake ice cover shows good agreement with that inferred from the satellite true color image, as well as the distribution of ice concentration. Ice concentration retrieved using MODIS data show better ice concentration distributions, e.g. over Lake Erie, than those from AMSR-E.

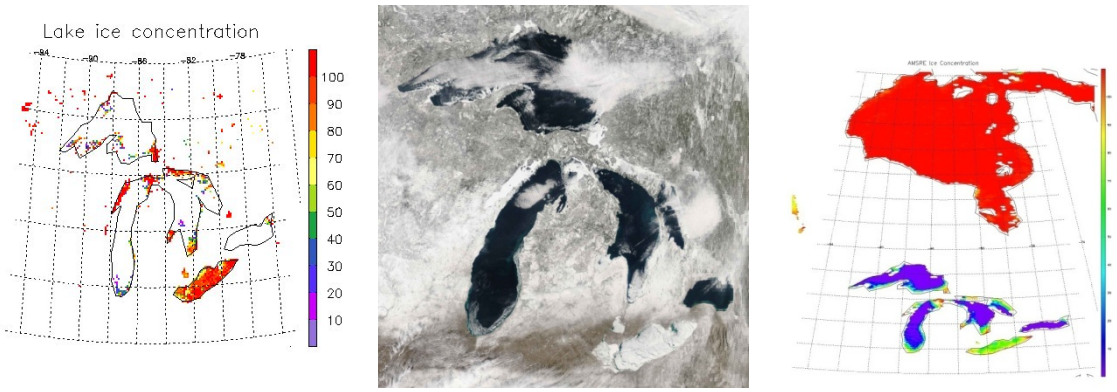

Figure 7. *Lake ice concentration (%) with MODIS Aqua data (left, MODIS true color image (middle), and ice concentration from AMSR-E (right) over Great Lakes on February 24, 2008.*

4.2.1.3 Comparison with ice chart

The Interactive Multisensor Snow and Ice Mapping System (IMS) began to generate daily snow and ice cover products at spatial resolution of 4 km in the Northern Hemisphere since 2004 in National Ice Center (http://nsidc.org/data/docs/noaa/g02156_ims_snow_ice_analysis/). This product has been used to validate the ice cover retrievals both over the Great Lakes and over the Arctic Ocean using this algorithm on MODIS data.

The bi-weekly ice charts generated in National Ice Center also provides Arctic ice concentration at spatial resolution of 25 km (http://nsidc.org/data/docs/noaa/g02172_nic_charts_climo_grid/index.html). This dataset has also been used to validate the ice concentration retrievals over the Arctic Ocean using this algorithm on MODIS data. Such ice chart data over the Great Lakes is currently unavailable.

4.2.2 Error Budget

Retrieved ice cover and concentration using MODIS data as proxy over the Arctic in 41 days evenly distributed in four seasons, and over the Great Lakes in similar number of days are compared with ice concentration product from AMSR-E, and ice chart as truth.

A pixel is determined as not ice covered if the AMSR-E sea ice concentration is lower than 15%. Comparisons show that the correct detection ratio of ice cover is 87.6% (Table 8), which is higher than the required measurement accuracy for ice cover. The bias and standard deviation of retrieved ice concentration are –4.0% (4.0%) and 25.6% (15.7%) over the Great Lakes (Arctic Ocean) compared with AMSR-E ice concentration (Table 9). Histogram of these two ice concentration differences is shown in Figure 10. Results show ice concentration retrievals using MODIS data as proxy meet the ice cover correct detection ration, 85%, and concentration accuracy and precision requirement, 10% and 30%, in comparison with AMSR-E product as truth. Further tuning of this algorithm, including ice detection test thresholds, new possible detection tests, and improvement in tie-point algorithm may be needed. Routine validation will be carried out over both sea and inland water. Also, quantitative validation of this algorithm will be conducted by comparing the derived ice cover and concentration with ice chart product, product from satellite instrument with higher spatial resolution, like Landsat.

***Table 12**: Performance of ice cover product compared with AMSR-E*

Case Number Total pairs: 1576298	Sea/Lake ice cover determined from AMSR-E	Water surface determined form AMSR-E
Sea/Lake ice cover determined using this algorithm	1075124	
Water surface determined using this algorithm		305872
Correct detection ratio = (1075124+305872)/1576298 = 87.6%		

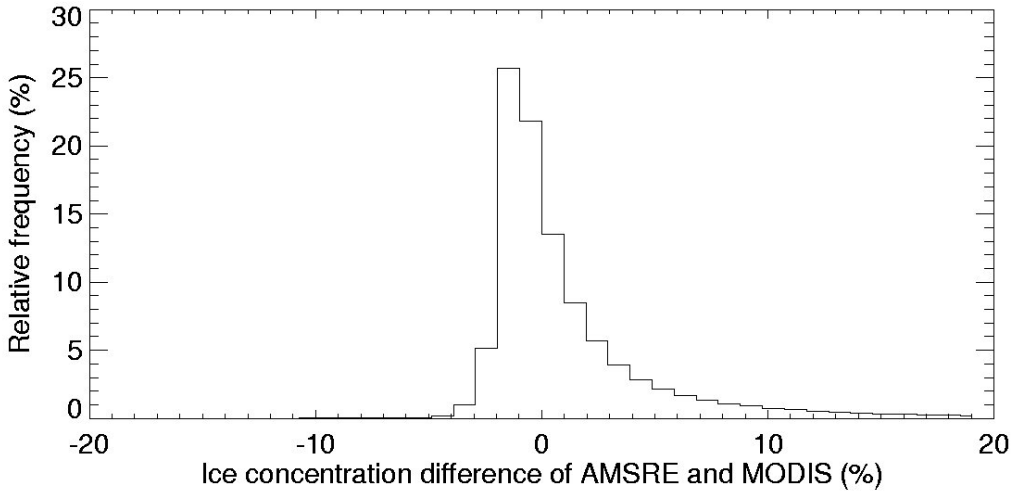

Figure 8. *Frequency distribution of ice concentration difference between AMSRE product and retrievals using this algorithm based on selected 41 clear day MODIS data in four seasons in 2007 over the Arctic Ocean.*

Table 13. *Performance of retrieved ice concentration compared with AMSR-E.*

Ice concentration difference of AMSR-E product and MODIS product as proxy of GOES-R ABI	Mean bias (%)	Standard Deviation (%)
Over Arctic Ocean	4.0	15.7
Over Great Lakes	-4.0	25.6
Required Measurement Accuracy	10	
Required Measurement Precision		30

Matches are found between retrieved ice concentration using this algorithm on MODIS data and ice chart over ten million for ice cover both over the Great Lakes and the Arctic Ocean, and over one hundred thousand for ice concentration over the Arctic Ocean. The results show that the correct detection ratio of ice cover is 91.5%, which is higher than the required measurement accuracy for ice cover. The bias and standard deviation of retrieved ice concentration are –1.2% and 9.5% (15.7%), which meets the ice concentration accuracy and precision requirement, 10% and 30%.

Further tuning of this algorithm, including ice detection test thresholds, new possible detection tests, and improvement in tie-point algorithm may be needed. Routine validation with AMSR-E, and ice chart will continue to be carried out over both sea and inland water. Quantitative validation of this algorithm will also be conducted by comparing the derived ice cover and concentration with product from satellite instrument with higher spatial resolution, like Landsat.

4.3 Validation of products using S-NPP VIIRS

This algorithm has been running using S-NPP VIIRS data. IST, ice concentration has been produced on each every overpass over both poles. Figure 9 shows the VIIRS IST on December 9, 2015 for one overpass over the Arctic and for a daily Arctic composite using all the overpasses in that day. Figure 10 shows the ice concentration on December 9, 2015 for one overpass and daily composite.

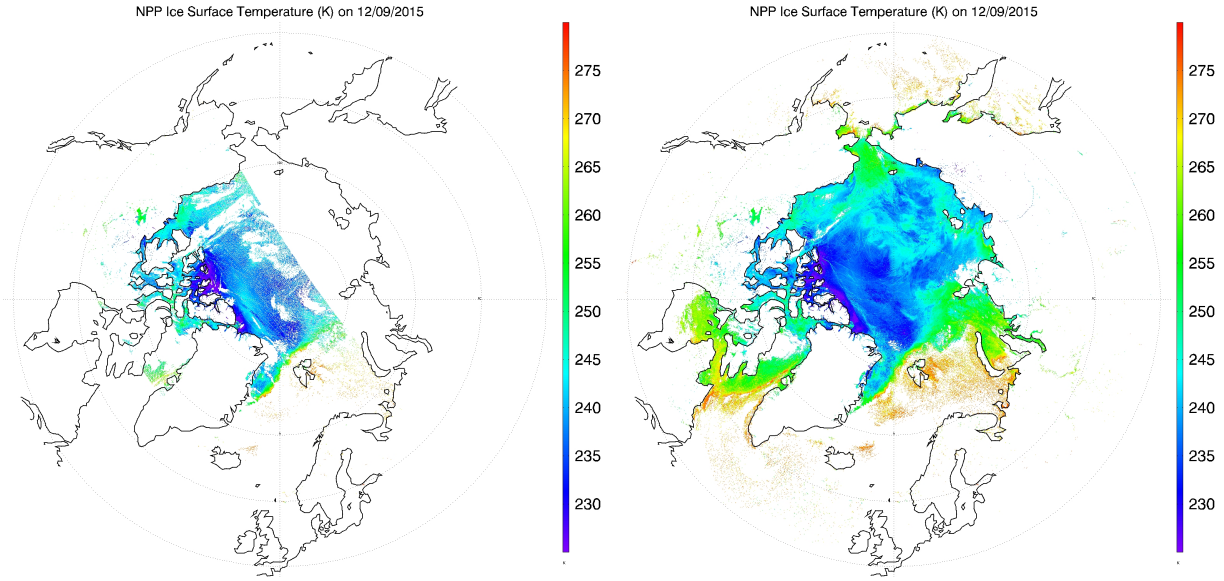

Figure 9. (left) Ice surface temperature (IST) for VIIRS overpass over the Arctic from 10:57 to 11:15 UTC on December 9, 2015; (right) daily IST composite over the Arctic on December 9, 2015.

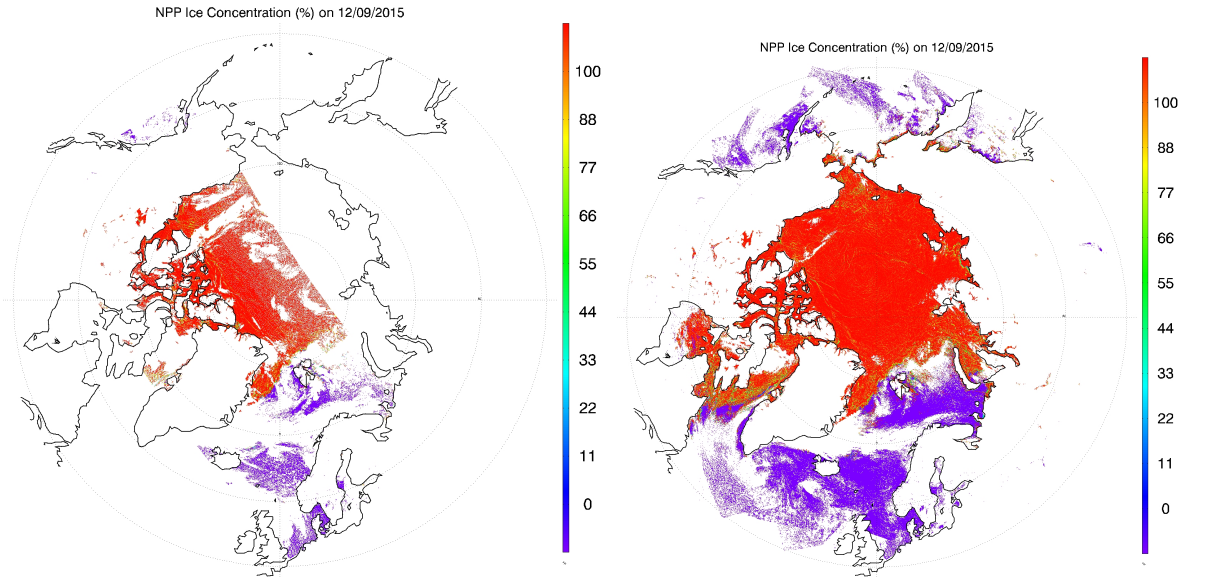

Figure 10. (left) Ice concentration for VIIRS overpass over the Arctic from 10:57 to 11:15 UTC on December 9, 2015; (right) daily ice concentration composite over the Arctic on December 9, 2015.

The quality of the S-NPP VIIRS IST has been being routinely examined and monitored. Validation is performed through comparisons with multiple datasets, including NASA IceBridge measurements, air temperature from Arctic drifting ice buoys, and MODIS IST. IST data sets from MODIS, specifically the Terra MODIS (MOD29) and Aqua MODIS (MYD29) Sea Ice Extent 5-Min L2 Swath 1 km datasets (Hall and Riggs 2015) are used to compare with the S-NPP VIIRS IST. These data sets are in swath format at 1 km resolution at nadir for both daytime and nighttime under clear sky conditions, with swath coverage of 2330 km (cross track) by 2030 km (along track). To collocate the VIIRS IST and MODIS IST, every overpass over the Arctic and Antarctic of the VIIRS IST and MODIS IST are re-gridded to a 1 km Equal-Area Earth Grid (EASE-Grid) using map projection tool MODIS Swath-to-Grid Toolbox (MS2GT) and compared, with 9025 by 9025 grid cells extending from 48.4 to 90°N over the Arctic and 8025 by 8025 grid cells extending from 53.2 to 90°S over the Antarctic. Only cases with VIIRS-MODIS observation time differences of less than 5 minutes are generated and shown for monitoring. Figure 11 shows the IST from MODIS Aqua and VIIRS on December 5, 2015, and both retrievals show similar pattern and values.

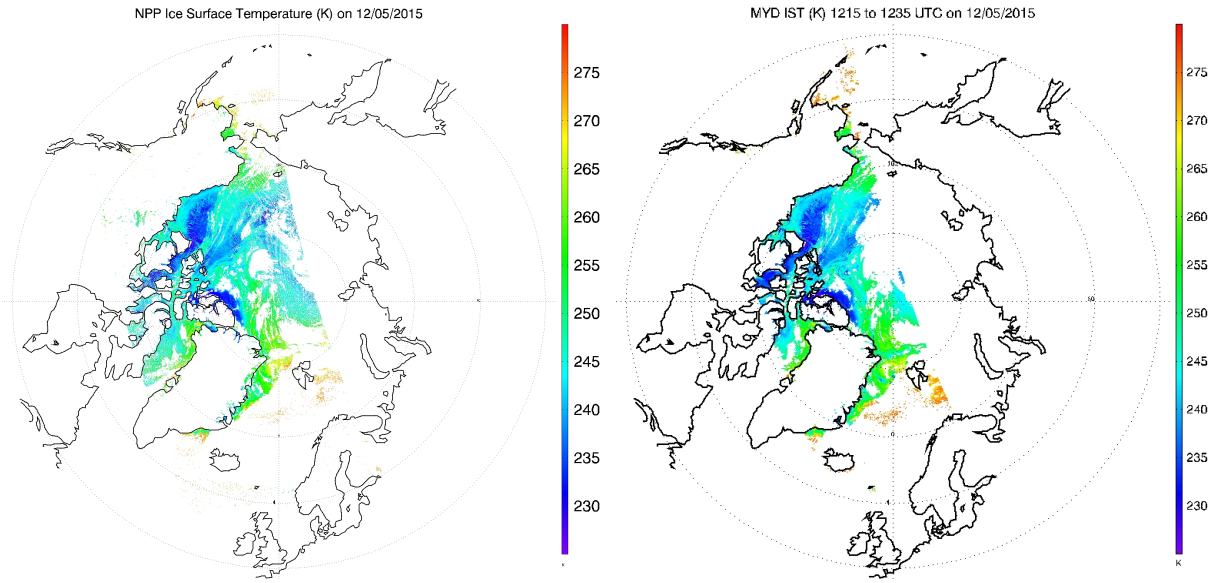

Figure 11. Ice concentration for VIIRS (left) from 12:13 to 12:31 UTC, and MODIS Aqua (right) from 12:15 to 12:35 UTC on December 5, 2015.

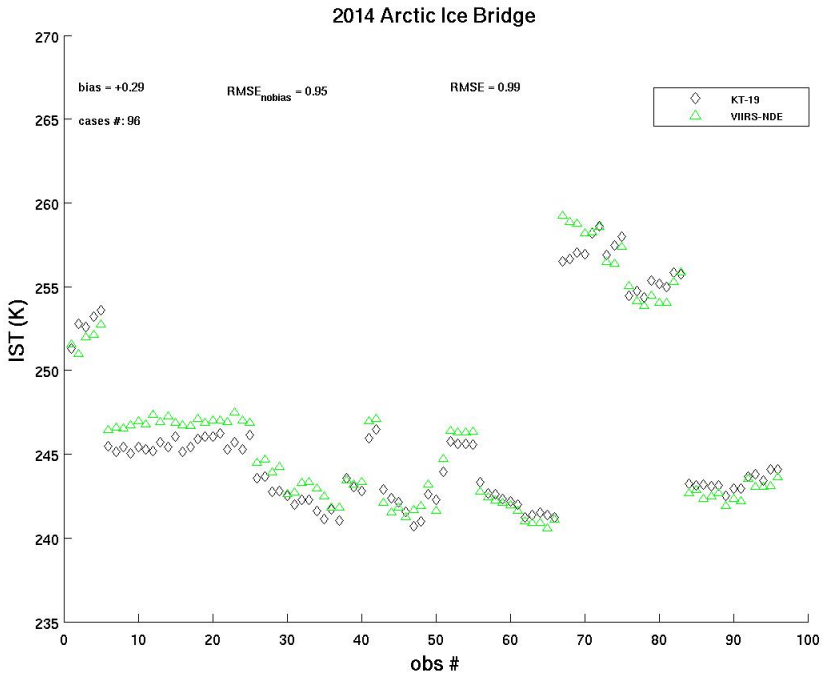

Figure 12. VIIRS IST (green) and KT-19 IST (black) for all coincident IceBridge flights with cloud-free observations over the Arctic (March-May 2014).

IST has been measured with an airborne Heitronics KT-19.85 Series II infrared radiation pyrometer (KT-19) on a National Aeronautics and Space Administration (NASA) P3 during the NASA Operation IceBridge campaigns (Krabill and Buzay 2014).The validation of the VIIRS IST with KT-19 IST measurements provides the most accurate assessment of VIIRS IST quality. All KT-19 observations in the Antarctic in 2012 and 2013, and in the Arctic in 2014, are used to validate collocated VIIRS IST. All available KT-19 temperature measurements that are within 375 m of the center of the VIIRS pixel are averaged. Only KT-19 temperature samples with standard deviations less than 1 K are used in matchup comparisons in order to eliminate cases with small-scale IST outliers that VIIRS would not be able to resolve. In addition, the closest KT-19 point to the VIIRS pixel must be within 15 minutes and 100 meters to be considered. Finally, a rigorous quality control is done to make sure that the VIIRS IST value is not contaminated by cloud. With 96 pairs of collocated VIIRS IST EDR and KT-19 IST over the Arctic and the Antarctic, the VIIRS minus KT-19 bias is 0.29 K, with an RMSE of 0.95 K (0.99 K) without (with) the bias included (Figure 12). It should be noted that the IceBridge KT-19 measurements are concentrated in the springtime. More measurements from other seasons, when the IST is near the melting point or is very low, are desirable.

The quality of the sea ice concentration and ice cover has been being monitored routinely and examined with other datasets. The quality of VIIRS sea ice concentration is being monitored using collocated sea ice concentration retrievals from the Special Sensor Microwave Imager/Sounder (SSMIS) onboard the Defense Meteorological Satellite (DMSP) F17 satellite processed with the NASA Team Algorithm (Cavalieri et al. 1999). This product contains daily

sea ice concentrations at a resolution of 25 km for both hemispheres. Sea ice concentration retrievals from VIIRS and the daily passive microwave product are collocated through remapping to a 25 km EASE-Grid with the nearest neighbor interpolation for the passive microwave data, and a weighted average for interpolation for VIIRS. An example of the collocated VIIRS and passive microwave sea ice concentration on December 9, 2015 is shown in Figure 13. Both products show similar overall spatial distributions, with VIIRS product shows more spatial details. A reduction in the sea ice concentration from the pack ice to the ice edge shown in the microwave product is not shown in the VIIRS product, which can partly be attributed to the differences in instrument sensitivities, instrument field-of-view, and the fundamental differences in the retrieval algorithms.

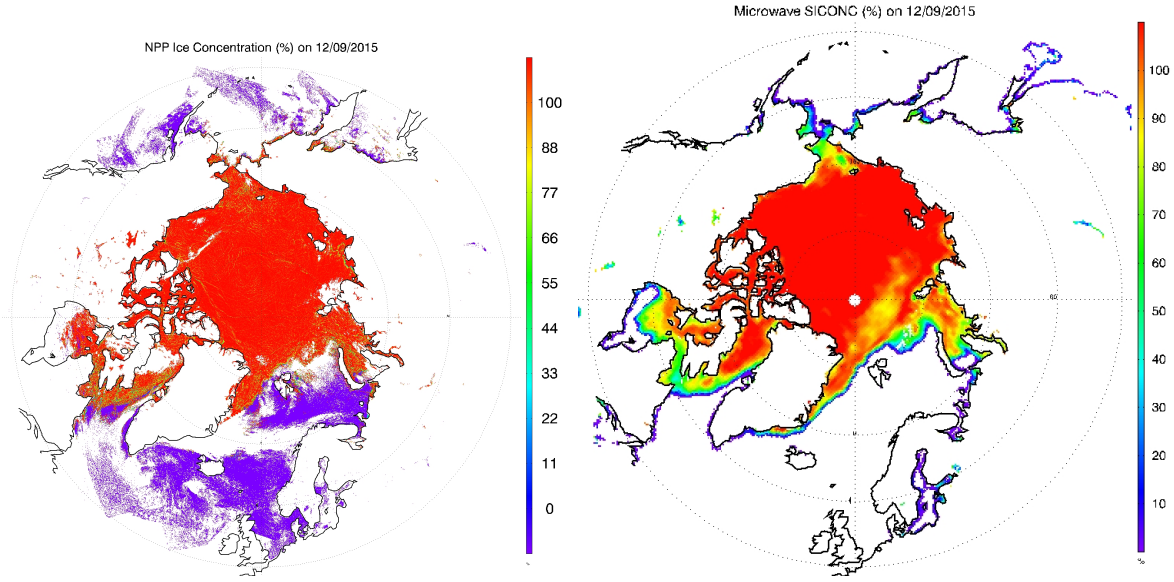

Figure 13. Ice concentration for daily ice concentration composite from VIIRS (left) and from microwave using NASA team algorithm (right) over the Arctic on December 9, 2015.

Validation of VIIRS sea ice concentration has been done by using high-resolution Landsat data. All Landsat 8 scenes in the year 2013 and 2014 that contain Arctic sea ice and are 90% or more clear sky covered are ordered from the U.S. Geological Survey (USGS) data sever. There are totally 181 Landsat scenes. In each scene, each pixel has visible and thermal channel observation at 30 m spatial resolution from the Operational Land Imager (OLI) and the Thermal Infrared Sensor (TIRS) onboard the Landsat 8. Each pixel at the original spatial resolution is identified as either snow/ice or water under clear conditions based on the visible channel reflectance and the derived NDSI. Sea ice concentration at lower spatial resolutions of 1 km, 6.25 km, and 25 km is calculated as the ratio of snow/ice pixel number to all pixel number inside a grid cell of 1 km, 6.25 km, and 25 km. For each of the Landsat scene, a correspondent S-NPP ice concentration with time difference less than 1 hour is collocated. Figure 14 shows a collocated Landsat ice concentration and S-NPP VIIRS ice concentration at 1 km spatial resolution. A daily mean sea ice concentration product is also sought from the Advanced Microwave Scanning Radiometer 2 (AMSR2) at 6.25 km, and from SSMIS at 25 km using NASA algorithm. These four SICs are

remapped to 6.25 km EASE-Grid (not for SSMIS). Bias and Root Mean Squared Error (RMSE) of ice concentration from the S-NPP VIIRS are calculated with regard to ice concentration from Landsat (Figure 15). The overall bias and precision of the S-NPP VIIRS ice concentration are 1.11% and 10.61% with validation with Landsat ice concentration.

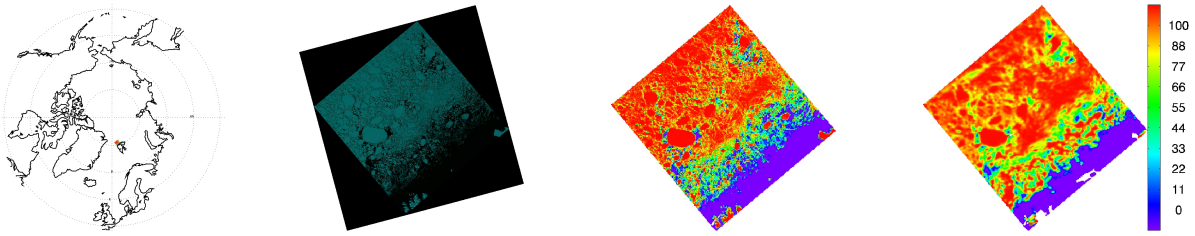

Figure 14. (from left to right) location of the scene shown; true color image of Landsat; Landsat sea ice concentration; and S-NPP VIIRS ice concentration at 12:09 UTC on May 27, 2013.

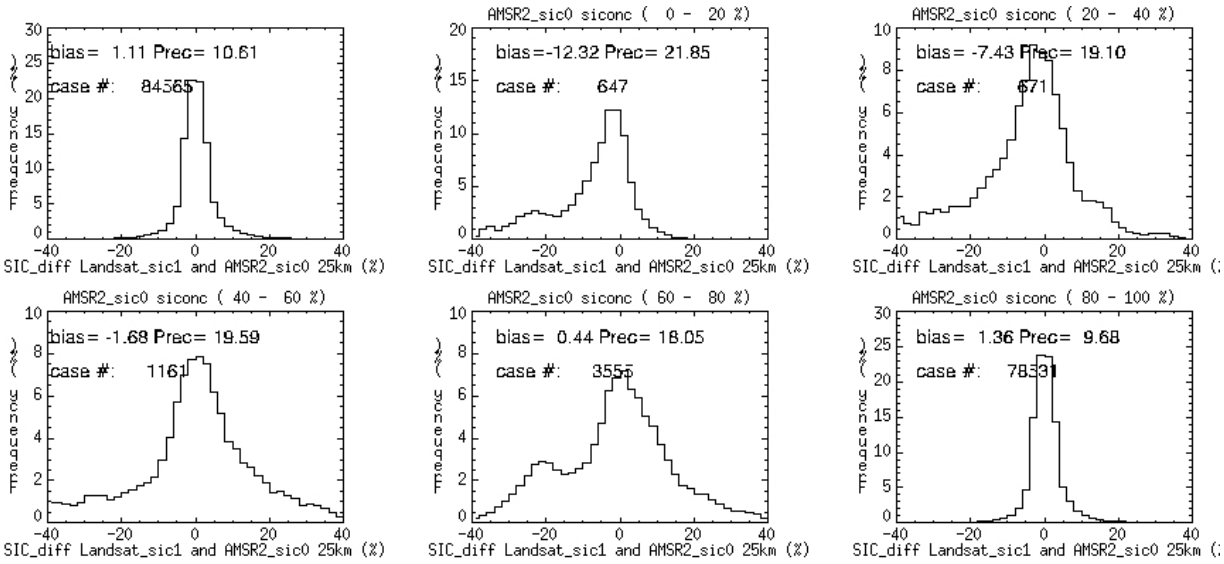

Figure 15. Comparison of VIIRS and Landsat ice concentrations for different concentration ranges/bins with bias and RMSE with bias removed (precision).

These validation and evaluation results demonstrate the high quality of the VIIRS IST and ice concentration as indicated by the absolute bias and RMSE values for the IceBridge KT-19 measurement, and Landsat ice concentration comparisons. Based on the IceBridge and Landsat results, the VIIRS IST and ice concentration uncertainty (RMSE and precision) meets or exceeds the JPSS system requirement.

5 Practical Considerations

5.1 Numerical Computation Considerations

This ice cover and concentration algorithm is implemented sequentially. The computation time is very economic.

5.2 Programming and Procedural Considerations

This ice cover and concentration algorithm requires spatial information distributions in a search window. Temporal information from previous observations is not necessary.

5.3 Quality Assessment and Diagnostics

Describe how the quality of the output products and the retrieval itself is assessed, documented, and any anomalies diagnosed.

The following procedures are recommended for diagnosing the performance of this algorithm.

- Check input data such as BTs, and reflectance for all pixels.
- Check the inputs from cloud mask, and land mask.
- Monitor the products automatically with other products from different satellite, and real time in-situ observations.
- Periodically image the individual test results to look for artifacts or non-physical behaviors.
- Maintain a close collaboration with other teams, which use the output of this algorithm in their product generation.

5.4 Exception Handling

This algorithm includes checking the validity of input data before running, and setting quality flag for the input data and in the output product. This algorithm also checks for missing input variables values. In this case, correspondent flag is set to indicate that no ice cover and concentration were produced for that pixel.

5.5 Algorithm Validation

This algorithm is validated using MODIS and SEVIRI data as proxy data, and using S-NPP VIIRS. Bias and standard deviation of ice concentration are calculated. Validations with other data sets show that this algorithm will meet the MRD required accuracy. More extensive

validation will be carried out using proxy data, MODIS, SEVIRI and other proxy data sets, over ocean and the inland waters, in comparison with ice products from AMSR-E, ice chart, and satellite instruments with very high spatial resolution.

6 Assumptions and Limitations

The following sections describe limitations and assumptions in the current version of this algorithm.

6.1 Assumptions

The following assumptions have been made in developing and estimating the performance of this algorithm. The following list contains the current assumptions and proposed mitigation strategies.

1. Cloud mask eliminates all possible cloud contamination.
2. Land mask maps are available to identify different surface types.
3. Changes of reflectance/temperature in each search window are mainly caused by difference in ice concentration on pixel level. Viewing angles in a search window do not change much considering the size of the search window. Pixels with 100% ice cover are majority in a search window.

We assume the sensor will meet its current specifications, and retrieved products from other teams will be accurate enough for this algorithm. This algorithm will be dependent on the following retrieved products.

- Surface skin temperature.

As for sensitivity estimates, a source error 0.5 K (0.01) in surface skin temperature (visible channel reflectance) leads to around 2% (2%) error in ice concentration, for tie point ice surface skin temperature (visible reflectance) being 250 K (0.55).

6.2 Limitations

Limitations of this algorithm includes

1. Ice concentration is not retrieved if less than 10% of all pixels in a search window is covered by ice, in which tie-point reflectance or surface temperature of pure ice can not be determined. However, ice cover can still be identified. Quality flags are set in the final ice concentration product for this condition.
2. The assumption that 100% ice cover pixels are majority in a search window can be violated under some conditions, when partially ice covered pixels are more than 100% ice

covered pixels, which might lead to uncertainties in the final ice concentration estimations.

6.3 Pre-Planned Product Improvements

Potential future improvements to the algorithm, the limitations they will mitigate, and possible and useful related information and links. This subsection should be organized into separate subsections for each potential enhancement, ordered according to a combination of highest operational priority and greatest feasibility in the next version.

This algorithm serves other applications. Its development is closely tied to the development and feedback from the other team algorithms. At this point, it is therefore difficult to predict what the future modifications will be. We intend to allow for feedback and to incorporate any suggestions from other teams to improve this algorithm.

7 References

Appel I., and J. A. Kenneth, 2002, Fresh water ice Visible/Infrared Imager/Radiometer Suite algorithm theoretical basis document, Version 5. SBRS document #: Y2404.

Bolsenga, S.J. 1983, Spectral reflectances of snow and fresh-water ice from 340 through 1100 nm. *J. Glaciology*, 29(102), 296-305.

Cavalieri, D. J., C. l. Parkinson, P. Gloersen, J. C. Comiso, and H. J. Zwally. 1999. Deriving Long-term Time Series of Sea Ice Cover from Satellite Passive-Microwave Multisensor Data Sets. *Journal of Geophysical Research* 104(7): 15,803-15,814.

Grenfell, T. C. and G. A. Maykut, 1977, The optical properties of ice and snow in the Arctic Basin, *J. Glaciol.*, 18, 445-63.

Hall, D. K. and G. Riggs. 2015. *MODIS/Terra Sea Ice Extent 5-Min L2 Swath 1km, Version 6*. Boulder, Colorado USA. NASA National Snow and Ice Data Center Distributed Active Archive Center. http://dx.doi.org/10.5067/MODIS/MOD29.006.

Hall, D. K. and G. A. Riggs. 2015. *MODIS/Aqua Sea Ice Extent 5-Min L2 Swath 1km, Version 6*. Boulder, Colorado USA. NASA National Snow and Ice Data Center Distributed Active Archive Center. http://dx.doi.org/10.5067/MODIS/MYD29.006.

Hall D.K., G.A. Riggs, and V.V. Salomonson, 2001, Algorithm theoretical basis document for the MODIS snow and sea ice mapping algorithms.

Hall D.K., G.A. Riggs, and V.V. Salomonson, 2006, MODIS sea ice products user guide to collection 5.

Key, J., J. Collins, C. Fowler, and R. Stone, 1997, High-latitude surface temperature estimates from thermal satellite data. Remote Sensing Environ., 61, 302-309.

Krabill, W.B.; Buzay, E. updated 2014. IceBridge KT-19 IR Surface Temperature, Version 1. [2012-2015]. **2012**, Boulder, Colorado USA. NASA National Snow and Ice Data Center Distributed Active Archive Center. http://dx.doi.org/10.5067/I883KXU7ZO8O

Lindsay, R. W., and D. A. Rothrock 1995, Arctic sea ice leads from advanced very high resolution radiometer images, J. Geophys. Res., 100, 4533-4544.

Riggs G.A., D.K. Hall, and S.A. Ackerman, 1999, Sea ice extent and classification mapping with the Moderate Resolution Imaging Spectroradiometer Airborne Simulator. Remote Sensing of Environ., 68, 152-163.

Schmit, Timothy J., Mathew M. Gunshor, W. Paul Menzel, James J. Gurka, Jun Li, A. Scott Bachmeier, 2005: INTRODUCING THE NEXT-GENERATION ADVANCED BASELINE IMAGER ON GOES-R. Bull. Amer. Meteor. Soc., 86, 1079-1096